Electronic Supplementary Material (ESI) for Catalysis Science & Technology.
This journal is © The Royal Society of Chemistry 2015

Supplementary Information

Electrocatalytic oxidation of water by a self-assembled oxo-vanadium(IV) complex modified gold electrode

Koushik Barman and Sk Jasimuddin*

Department of Chemistry, Assam University, Silchar, Assam-788011

Experimental

[VO(acac)$_2$], 4-aminothiophenol and isonicotinic acid ware purchased from Sigma Aldrich. 0.1M phosphate buffer solution (PBS) was prepared by mixing 0.1 M $NaClO_4$ and 0.01 M H_3PO_4 and the pH's were adjusted by the addition of 0.11 M NaOH using Smalley's method[1]. Double distilled water was used throughout the course of the experiment. The field emission scanning electron microscopy (FE-SEM) images were obtained using FE SEM, FEI INSPECT F50 operated at an acceleration voltage of 20 kV. Electrochemical measurements were performed on a CHI 660C Electrochemical workstation (CH Instrument, USA). A three electrode system was employed with gold or modified gold electrode as working electrode, Pt wire as a counter electrode and Ag/AgCl (3M KCl) as reference electrode. The pH measurements of solutions were carried out on a pH meter (Macro Scientific Works (Regd), New Delhi). Controlled potential electrolysis was performed in a stirred 0.1 M PBS solution (pH 7.0) in a gas-tight electrochemical cell. All experiments were performed at ambient temperature and inert atmosphere. The turn over frequency (TOF) was calculated from the steady-state current obtained from controlled potential electrolysis.The Faradaic efficiency of the catalyst was measured by a three-electrode electrochemical cell system, where oxygen was rapidly produced on the surface of the modified gold electrode after initiating electrolysis at 0.89 V. A calibrated Ocean Optics FOXY probe was used for oxygen measurement. The Faradaic efficiency was calculating using the relation, Faraday efficiency (%) = (Amount of O_2 × Number of electrons needed to produce O_2) / amount of charge passed to solution.

Electrode modification Process

1. Electrode pre-treatment and immobilization of 4-(pyridine-4$^{/}$-amido)thiophenol (4-PATP) on gold electrode

A gold electrode (2 mm in diameter) was polished with aqueous slurries of α-alumina (0.5 μm) on a polishing pad and rinsed extensively with ethanol and distilled water. The mechanically cleaned electrode was electrochemically cleaned in 0.5 M H_2SO_4 until a steady characteristic gold oxide cyclic voltammogram was obtained[2]. The clean gold electrode was immersed into the 1.0 mM ethanolic solution of 4-aminothiophenol for 24 hours. The 4-ATP was self-assembled over the gold electrode surface via gold-sulfur interaction and the modified electrode was thoroughly washed with water and distilled water. Thereafter, the 4-ATP-Au electrode was dipped into an isonicotinic acid solution (1.0 mM) for 4 hours under stirring condition. The 4-(pyridine-4$^{/}$-amido)thiophenol modified gold electrode (4-PATP-Au) was formed and washed with distilled water for further modification.

2. Complexation of [VO(acac)$_2$] on 4-PATP-Au electrode

4-PATP-Au electrode was immersed into an ethanolic solution of [VO(acac)$_2$] (1×10^{-3} M) and stirred for 2 hours. Pyridine nitrogen of 4-PATP-Au was coordinate with the vacant coordination site of vanadium in [VO(acac)$_2$]. After adduct formation, the finally modified electrode ([VO(acac)$_2$]-4-PATP-Au) was washed thoroughly with distilled water and dried in air for further use.

Characterization of modified gold electrode

The stepwise modification process (scheme 1) was monitored by cyclic voltammetry and electrochemical impedance spectroscopy using $[Fe(CN)_6]^{3-/4-}$ as redox probe in 0.1 M PBS solution at pH 7.0. The cyclic voltammogram of 0.5 mM $[Fe(CN)_6]^{4-}$ exhibits an electrochemically reversible redox couple on bare electrode. After modification the gold electrode with 4-ATP (4-aminothiophenol), the cyclic voltammogram of $[Fe(CN)_6]^{4-}$ exhibit an irreversible couple with low current height than bare gold electrode. The current height decreased even more when 4-(pyridine-4$^{/}$-amido)thiophenol (4-PATP) modified Au was used as working electrode. These CV results (Figure S1) indicate that the electronic communication between gold and $[Fe(CN)_6]^{4-}$ is blocked due to 4-PATP film formation. The surface coverage ($\theta = 0.98$) was obtained by using $\theta = [1-(i_p/i_p^0)]$, where i_p^0 (3.761×10^{-5} μA) and i_p (6.227×10^{-7} μA) are peak currents of the redox probe at bare and 4-PATP modified gold electrode, respectively under similar conditions[3]. Electrochemical impedance spectroscopy supports the CV results. In the Nyquist plot, the diameter of the semi-circle increases gradually when stepwise modification on the gold electrode surface was carried out. The observed trend is due to the fact that the modified electrode blocked the electron transfer for the redox reaction of $[Fe(CN)_6]^{4-}$. The surface coverage ($\theta = 0.95$) was estimated by using the relation $\theta = [1- (R_{ct}^0/R_{ct})]$ where R_{ct}^0 (12.11×10^6 Ω) and R_{ct} (2.496×10^8 Ω) are the charge transfer resistance of the redox probe at bare Au and 4-PATP-Au electrode.[3]

Table S1 Comparative account of different electrochemical water oxidation catalyst

Catalyst (electrode)	Overpotential (V) *vs* NHE at J (mA/ cm^2)	TOF (s^{-1}) at η (V)	pH	Reference
Mn oxide film (ITO coated Glass plate)	0.59 (1.00)	0.01 (0.53)	7.0	[4]
$Mn_3(PO_4)_2.3H_2O$ (FTO)	0.68 (0.32)	0.001 (0.68)	7.0	[5]
Fe based thin film (ITO)	0.48 (1.00)	0.21 (0.53)	7.0	[6]
Co(II)ion (ITO)	0.55 (1.00)	0.02 (0.53)	7.0	[4,7]
Ni-B_i film (GC)	0.54 (1.00)	0.01 (0.53)	9.2	[4, 8]
NiO_x-en (FTO)	0.51 (1.00)	0.02 (ca.0.61)	9.2	[9]
$[Ni_{1-x}Fe_x(OH)_2](NO_3)_y(OH)_{x-y}\cdot nH_2O$ (Flat HOPG)	0.26(10.00)	-	-	[10]
Co_3O_4 nanoparticles (Flat HOPG)	0.31 (0.50)	0.21 (0.34)	14	[11]
Thin-film solution-cast $Ni_{0.9}Fe_{0.1}O_x$ (Au/Ti-coated quartz crystal)	0.34 (10.00)	-	14	[12]
$NiFeAlO_4$ inverse spinel (GC)	0.41 (0.10)	-	13	[13]
Cobalt−salen complexes (FTO)	0.29 (0.01)	-	9.2	[14]
$[Ru(bpy)]_5[Ru_4POM]$ thin film (GC)	0.49 (0.55)	0.35 (0.49)	7.0	[15]
Carbon grafted Ir Complex (Carbon)	0.66 (0.05)	3.30 (0.66)	5.0	[16]
Cobalt (II) (FTO)	0.80 (0.16)	4.00 (0.80)	7.2	[17]
$[VO(acac)_2]$-4-PATP (Au)	0.28 (3.82)	0.64 (0.28)	7.0	[Present work]

POM: Polyoxometalates

The overpotential (η) for water splitting was calculated using the relation,

$\eta = E\ (NHE)_{measured} - E\ (NHE)_{thermodynamic}$

where, $E(NHE)_{measured} = E\ (Ag/AgCl) + 0.210\ V$ and

$E\ (NHE)_{thermodynamic} = E^0 - 0.059 \times pH = (1.229 - 0.059 \times pH)\ V$ at 25 °C.

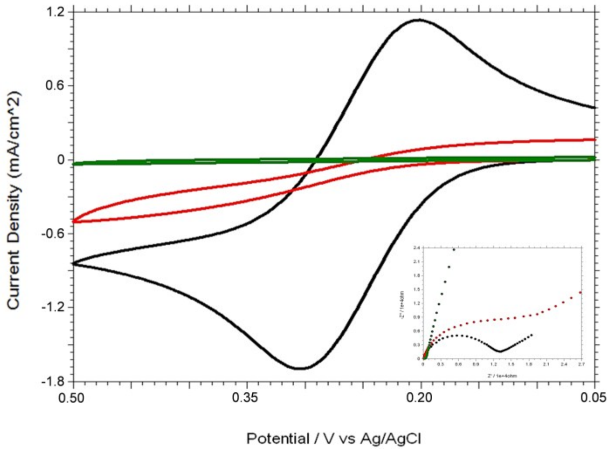

Figure S1 Overlaid cyclic voltammogram and Nyquist plot (-Z$^{//}$ versus Z$^{/}$) (inset) of 0.5 mM $[Fe(CN)_6]^{4-}$ in 0.1 M PBS solution at pH 7.0 using different working electrode [bare Au (black), 4-ATP-Au (red) and 4-PATP-Au (green)]

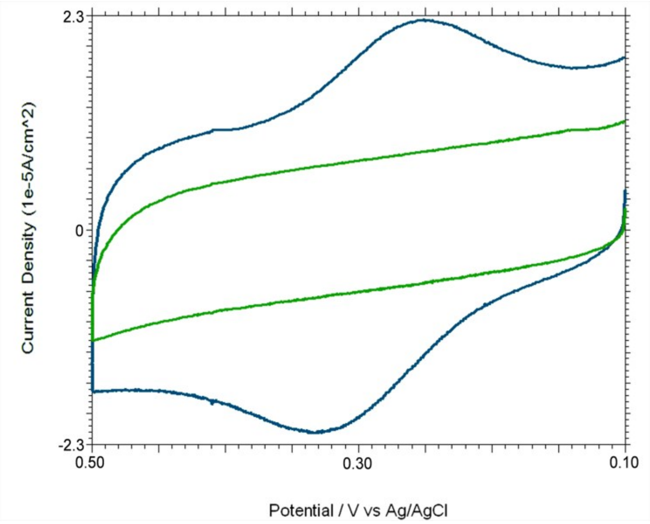

Figure S2 Cyclic voltammograms obtained from $[VO(acac)_2]$-4-PATP (blue) and 4-PATP (green) modified gold electrode in 0.1 M PBS buffer at pH 7.0. (Scan rate: 100 mV s^{-1})

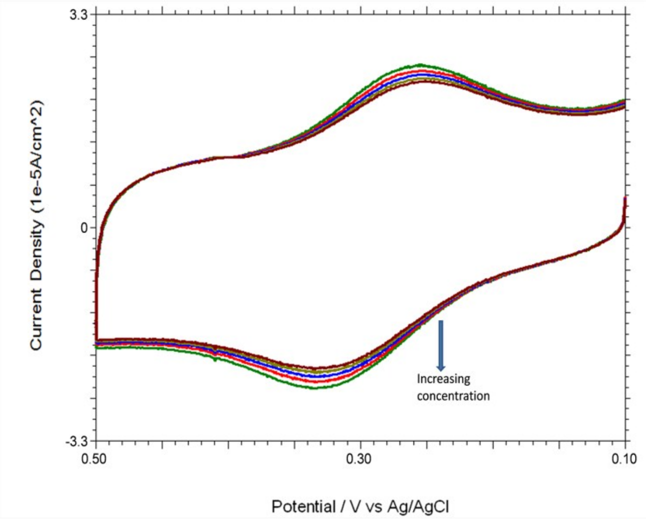

Figure S3 Cyclic voltammograms obtained from 4-PATP modified gold electrode in varying concentration (1.0 – 5.0 mM) of [VO(acac)$_2$] solution.

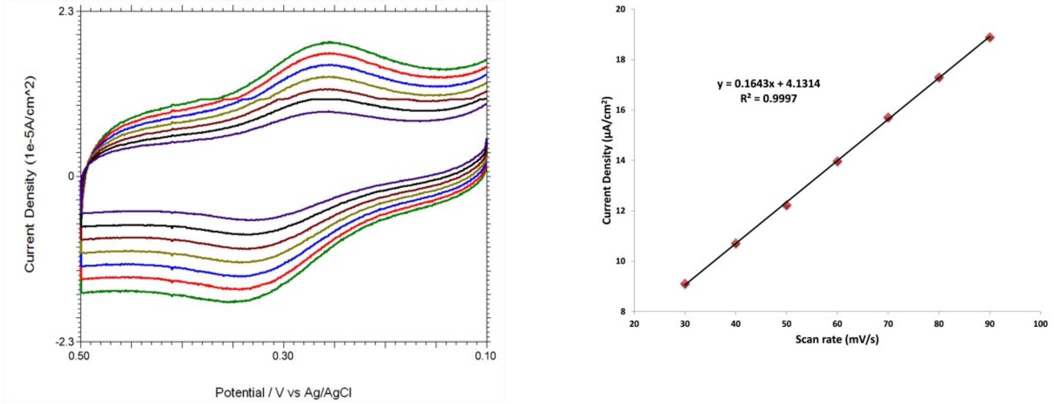

Figure S4 Cyclic voltammograms obtained with [VO(acac)$_2$] complex modified gold electrode in 0.1 M PBS at different scan rates (30-90 mV/s) at pH 7.0 and (b) (right): Plot of scan rate *versus* current density (j$_{pc}$).

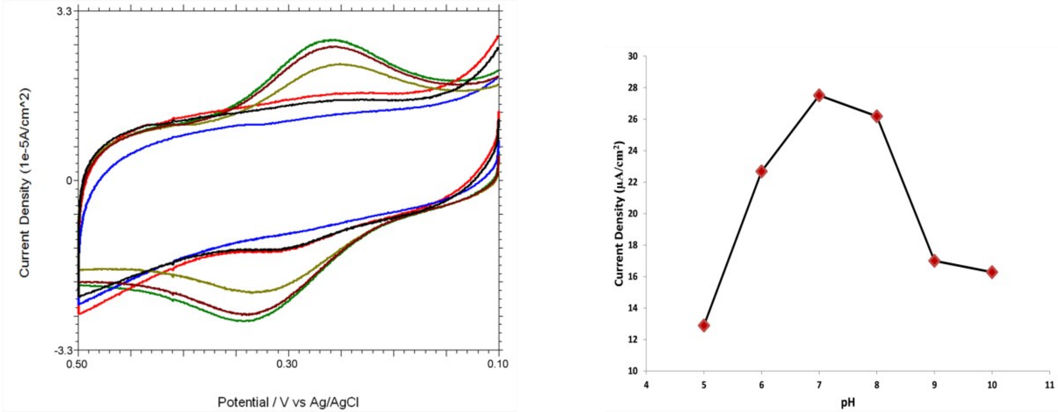

Figure S5 (a) Cyclic voltammogram of [VO(acac)$_2$]complex electrode surface at different pH 5.0(blue), 6.0(light green), 7.0(dark green), 8.0(brown), 9.0(red) and 10.0(black) and (b) Plot of pH versus current.

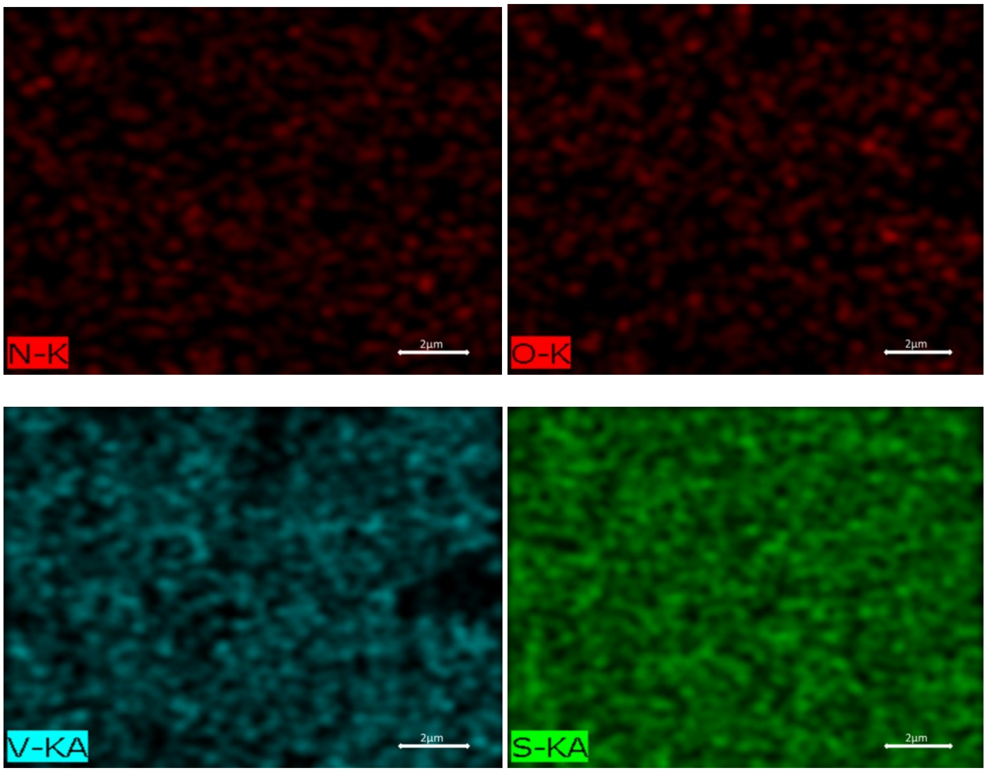

Figure S6 Elemental mapping images of nitrogen, oxygen, sulphur and vanadium corresponding to the SEM image of [VO(acac)$_2$]-4-PATP-Au electrode.

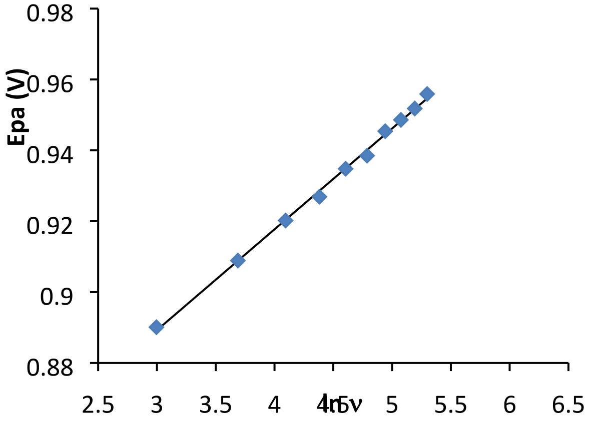

Figure S7 A plot of anodic peak potential (E_{pa}) *versus* lnν.

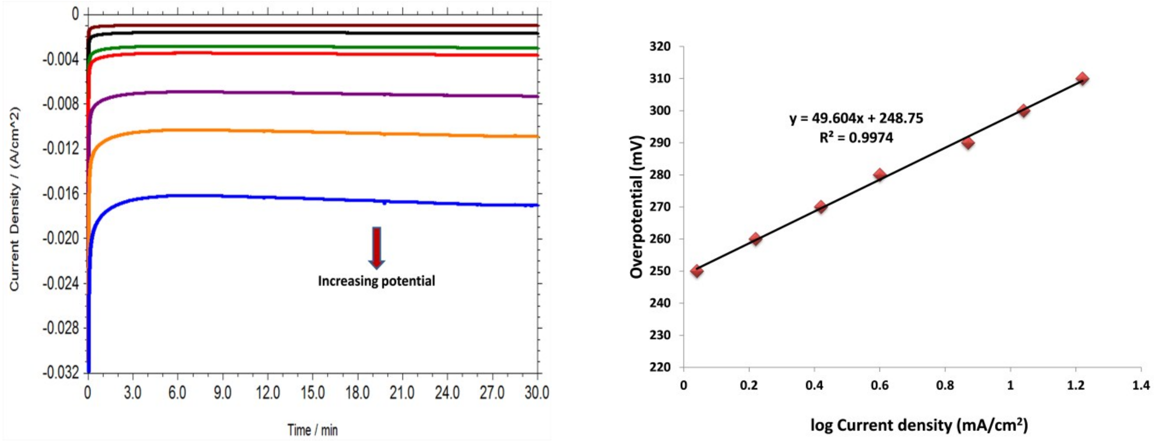

(a) (b)

Figure S8 (a) Current density *versus* time plot as the applied potential is stepped from 0.86 to 0.92 V. (b) Tafel plot of [VO(acac)$_2$]-4-PATP modified gold electrode in 0.1 M PBS (pH 7.0) at different applied potential. The slope of the graph is around 50 mV per decade.

All data were collected with iR compensation. Stable currents were measured at applied potential ranging from 0.86 to 0.92 V at every 10 mV step for 30 minutes controlled potential electrolysis with stirring. A steady state was obtained at every particular potential with currents ranging from 1.0 to15.8 mA/cm^2.

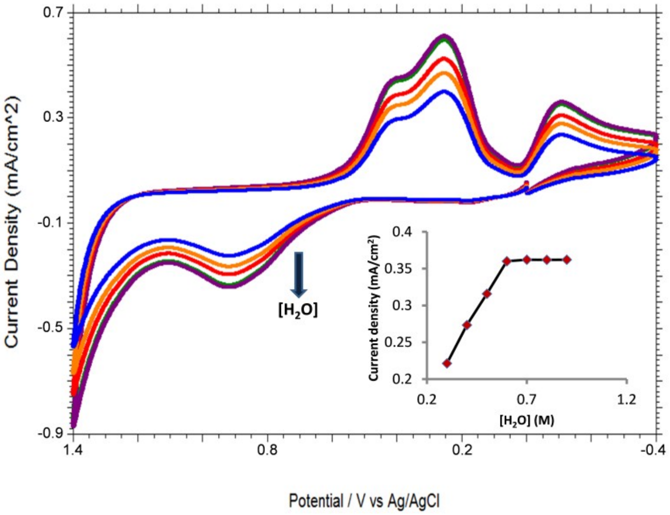

Figure S9 Cyclic voltammograms obtained from [VO(acac)$_2$]-4-PATP modified gold electrode with increasing amount of [water] (0.3 to 0.9 M). Inset: A plot of anodic peak current density *versus* [H$_2$O].

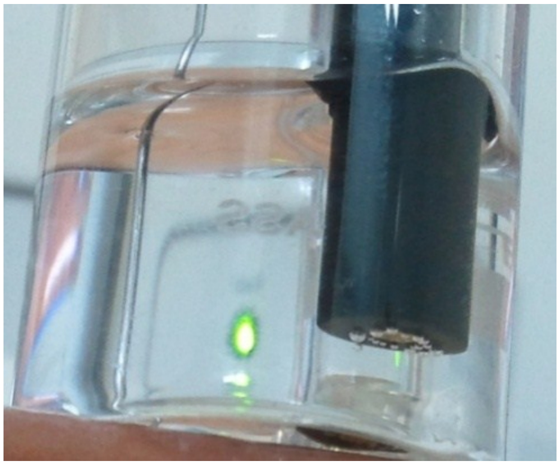

Figure S10 Photo taken after the potential was cycled seven times between -0.4 to 1.4 V versus Ag/AgCl at a scan rate of 100 mV s^{-1} on the [VO(acac)$_2$]-4-PATP modified gold electrode with 0.1 M PBS solution (pH 7.0).

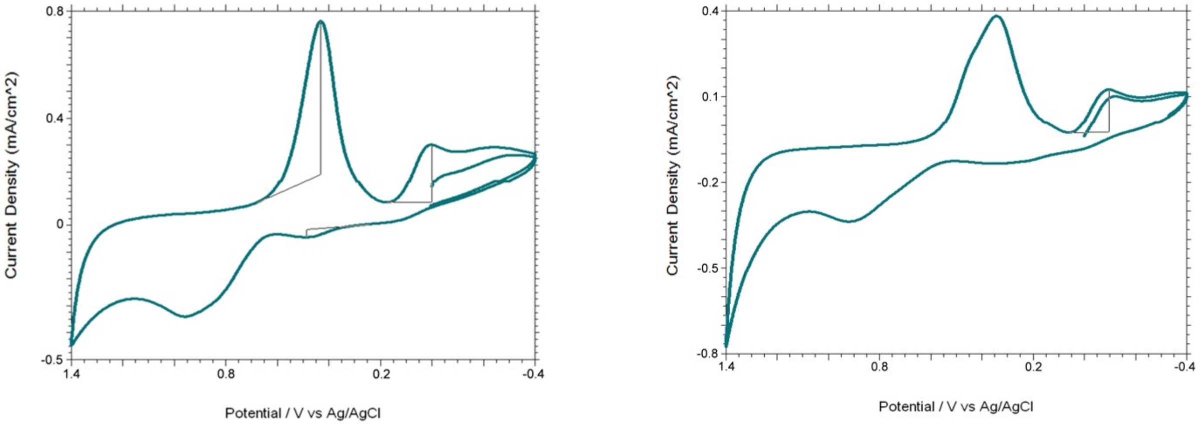

(a)

(b)

Figure S11 Cyclic voltammogram obtained with [VO(acac)$_2$]-4-PATP-Au electrode in 0.1 M phosphate buffer solution (a) sweeping the potential negatively first in the absence of O$_2$ and then sweeping the potential positively and then negatively; (b) Sweeping the potential negatively in the presence of O$_2$ and then sweeping the potential positively and then negatively in the presence of O$_2$.

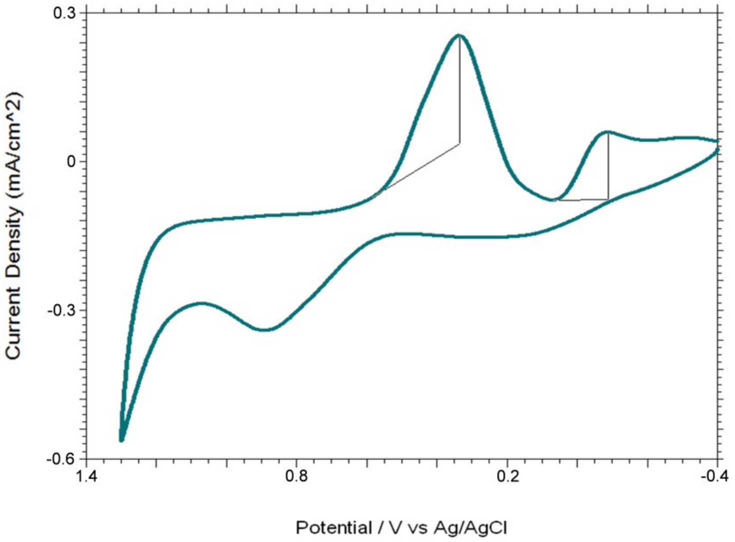

Figure S12 Cyclic voltammogram obtained with [VO(acac)$_2$]-4-PATP-Au electrode in acetate buffer solution (pH = 7.0).

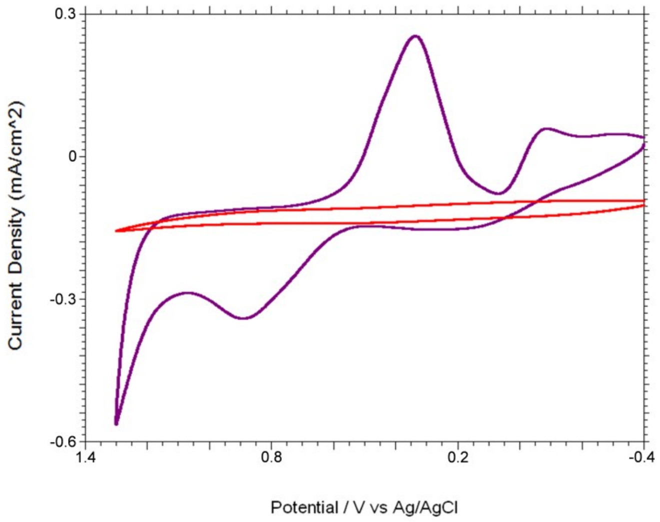

Figure S13 Cyclic voltammogram obtained with [VO(acac)$_2$]-4-PATP-Au electrode in CH_3CN containing 0.1 M [Bu_4N][ClO_4] (pH = 6.6) (red curve) and in CH_3CN + H_2O mixed solvent containing 0.1 M [Bu_4N][ClO_4] (pH = 7.0) (violet curve).

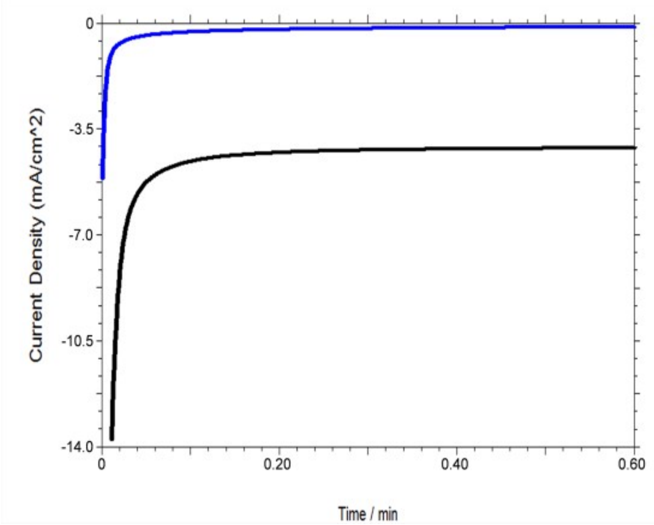

Figure S14 Enlarged plot of Figure 4 (Bulk electrolysis with (black curve) and without (blue curve) the [VO(acac)$_2$] catalyst over the 4-PATP-Au electrode in 0.1 M phosphate buffer (pH 7.0) at 0.89 V *versus* Ag/AgCl)

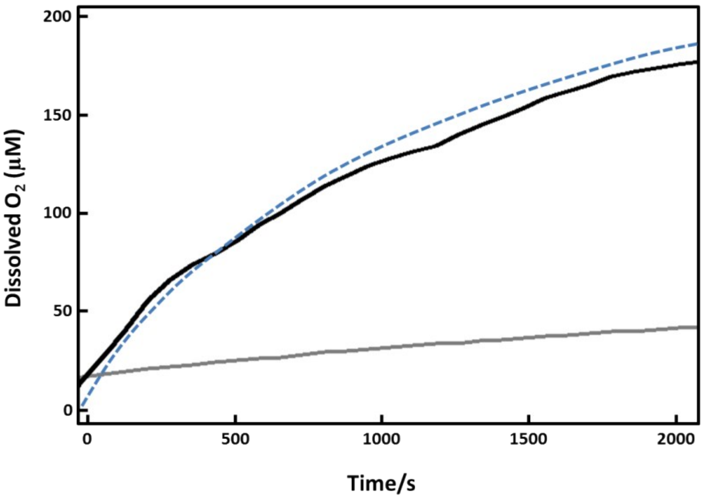

Figure S15 Oxygen evolution during the controlled potential electrolysis of water in a gas-tight electrochemical cell in N_2 atmosphere (PBS buffer, pH 7.0) without (gray curve) and with (black curve) the [VO(acac)$_2$] catalyst as measured with a fluorescence probe. Dotted line shows the theoretical oxygen evolution with 100% efficiency.

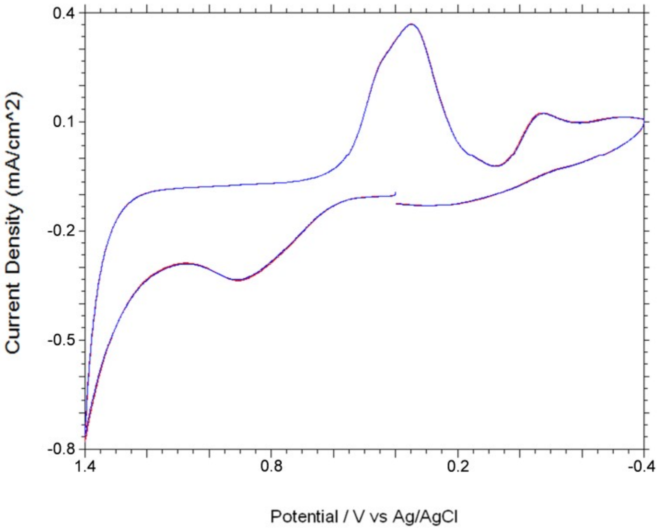

Figure S16 Overlaid cyclic voltammograms obtained with [VO(acac)$_2$]-4-PATP-Au electrode in 0.1 M PBS (pH 7.0) for 15 days intervals (up to 30 days).

References

1. J. F. Smalley, K. Chalfant, S. W. Feldberg, T. M. Nahir, E. F. Bowden, *J. Phys. Chem. B*. 1999, **103**, 1676.
2. R. K. Shervedani, A. Hatefi-Mehrjardi, M. KhosraviBadadi, *Electrochim. Acta*, 2007, **52**, 7051.
3. R. K. Shervedani, S. M. S. Barzoki, M. Bagherzadeh, Electroanalysis, 2010, **22**, 969.
4. I. Zaharieva, P. Chernev, M. Risch, K. Klingan, M. Kohlhoff, A.Fischer, H. Dau, *Energy Environ. Sci*. 2012, **5**, 7081.
5. K. Jin, J. Park, J. Lee, K. D. Yang, G. K. Pradhan, U. Sim, D. Jeong, H. L. Jang, S. Park, D. Kim, N. E. Sung, S. H. Kim, S. Han, K. T. Nam, *J. Am. Chem. Soc*. 2014, **136**, 7435.
6. Y. Wu, M. Chen, Y. Han, H. Luo, X.Su, M-T. Zhang, X. Lin, J. Sun, L. Wang, L. Deng, W. Zhang, and R. Cao. *Angew. Chem. Int. Ed*. 2015, **54**, 4870.
7. M. W. Kanan, D. G. Nocera, *Science* 2008, **321**, 1072.
8. M. Dinca˘, Y. Surendranath, D. G. Nocera, *Proc. Natl. Acad. Sci.*USA 2010, **107**, 10337.
9. A. Singh, S. L. Y. Chang, R. K. Hocking, U. Bach, L. Spiccia, *Energy Environ. Sci*. 2013, **6**, 579.
10. B. M. Hunter, J. D. Blakemore, M. Deimund, H. B. Gray, J.R. Winkler, and A. M. Müller *J. Am. Chem. Soc*., 2014, **136**, 13118.
11. J. D. Blakemore, H. B.Gray, J. R. Winkler, A. M. Müller, ACS Catal., 2013, **3**, 2497.
12. L. Trotochaud, J. K. Ranney, K. N. Williams, S. W. Boettcher, *J. Am. Chem. Soc.,* 2012, ***134***, 17253.
13. J. Y. C. Chen, J. T. Miller, J. B. Gerken, S. S. Stahl, *Energy Environ. Sci.* 2014, *7*, 1382.
14. H. Chen, Z. Sun, X. Liu, A.Han, and P. Du, *J. Phys. Chem. C*., 2015, **119**, 8998.
15. S. -X. Guo, C-Y. Lee, J. Zhang, A. M. Bond, Y. V. Geletii, C. L. Hill, *Inorg. Chem*., 2014, **53**, 7561.
16. K. E. Dekrafft, C. Wang, Z. Xie, X. S. Su, B. J. Hinds, W. Lin, *Acs. Appl. Mater. Interfaces*, 2012, **4**, 608.
17. C. A. Kent, J. J. Concepcion, C. J. Daves, D. A. Torelli, A. J. Rieth, A. S. Miller, P. G. Hoertz, T. J. Meyer, *J. Am. Chem. Soc*., 2013, **135**, 8432.